Student thesis series INES nr 593

Changes in July albedo and its relationship with EVI over the last two decades in the Swedish alpine region

Vera Grönvik Hende

2023
Department of
Physical Geography and Ecosystem Science
Lund University
Sölvegatan 12
S-223 62 Lund
Sweden

Vera Grönvik Hende (2023).
Changes in July albedo and its relationship with EVI over the last two decades in the Swedish alpine region
Bachelor degree thesis, 15 credits in **Physical Geography and Ecosystem Analysis**
Department of Physical Geography and Ecosystem Science, Lund University

Level: Bachelor of Science (BSc)

Course duration: *January* 2023 until *June* 2023

Disclaimer

This document presents work undertaken as part of a study program at Lund University.

Changes in July albedo and its relationship with EVI over the last two decades in the Swedish alpine region

---

Vera Grönvik Hende

Bachelor thesis, 15 credits, in **Physical Geography and Ecosystem Analysis**

Supervisor:
David Tenenbaum
Lund University

Exam committee:
Karin Larsson, Lund University
Thomas Holst, Lund University

Acknowledgements

Thanks to my supervisor David Tenenbaum for valuable advice and input during the writing of this thesis. I also want to thank my friends for their support and patience with me during the writing process.

Abstract

Vegetation in the subarctic is expected to respond to climate warming as its growth becomes less temperature limited. This has previously been recorded in the form of treeline advances and increasing shrub cover. Changes in vegetation cover may accelerate warming due to a decrease in summer albedo, in what is termed surface albedo feedback. A quantification of the relationship between vegetation change and its corresponding change in surface albedo is therefore important to better understanding of the surface energy balance and its consequent impacts on the climate. This study focuses on the Swedish portion of the Scandes mountain range and its surrounding area and set out to investigate whether the shortwave albedo in July has changed significantly in this region between the years 2000 to 2022, and whether this corresponds to a change in vegetation. This was done by using imagery from the Moderate Resolution Imaging Spectroradiometer (MODIS). Vegetation changes were quantified using the Enhanced Vegetation Index (EVI). Changes in both shortwave albedo and EVI were quantified using a linear regression model and their relationship was assessed through correlation analysis. This study found, contrary to expectations, that the shortwave albedo for July had mainly been stable or increased. Significant ($p<0.05$) trends in shortwave albedo changes were found for 44% of the area, of which 79% were increasing trends. Out of the area with significant changes in shortwave albedo, 38% had also a significant ($p<0.05$) change in EVI, most of which (83%) were increasing trends in EVI as well. The correlation between shortwave albedo and EVI for the entire area was, however, quite weak ($\rho=0.227$) but showed varying correlation strength when considering vegetation classes separately. Vegetation below the treeline had a positive relationship between shortwave albedo and EVI, whereas vegetation above the treeline in some areas had a negative trend in EVI, indicating possible vegetation browning, along with a corresponding increasing trend in shortwave albedo. The mechanisms behind the changes in shortwave albedo throughout the Swedish alpine region remain ambiguous, and the differences in trends for the different vegetation classes suggest a need for a closer look at specific species responses within each subregion of the Scandes vegetation classes.

Keywords: shortwave albedo, Enhanced Vegetation Index (EVI), alpine vegetation, Scandes, surface albedo feedback, MODIS

Table of Contents

1. Introduction *1*

1.1 Background 1

1.2 Aim of study 2

1.3 Study area 3

2. Method *4*

2.1 Data acquisition and processing 4

2.2 Analysis 5

3. Results *6*

3.1 Albedo 6

3.2 EVI 7

3.3 Albedo and EVI relationship 8

3.4 Vegetation class comparison 9

3.5 Time series outlier evaluation 13

4. Discussion *15*

4.1 Albedo and EVI were mostly stable or increasing 15

4.2 Albedo and EVI correlations 18

4.3 Method limitations 19

4.4 Considerations for future studies 20

5. Conclusion *21*

6. References *22*

1. Introduction

1.1 Background

High latitudes are showing a more pronounced warming as compared to the rest of the globe (Box et al., 2019; Pithan & Mauritsen, 2014; Serreze & Barry, 2011). This process is termed arctic amplification, and has been identified to be caused by a multitude of complex processes occurring at different scales (Cohen et al., 2014; Serreze & Barry, 2011). One of these processes is the decrease of highly reflective snow and ice cover, as these regions melt due to climate warming, thereby exposing darker, less reflective areas and producing a positive feedback effect (Serreze & Barry, 2011). The reflective properties of a surface are termed albedo, which is a dimensionless quantity measured from 0 to 1, with 0 being a blackbody which absorbs all incoming radiation, and 1 being a perfect reflector. The land surface albedo is an important variable in the shortwave radiation balance and interacts with climate variability through various mechanisms (Liang & Wang, 2019). In order to understand the drivers behind the amplified warming in high latitude areas it is therefore important to quantify and increase our knowledge of the mechanisms behind changes in surface albedo.

Shortwave surface albedo has been widely measured using satellite remote sensing, although the process is not inherently straightforward as it is must take into account properties of the surface as well as atmospheric conditions. This is typically done by using a bidirectional reflectance distribution function (BRDF), which provides a mathematical description of the reflectance of the surface (Liang & Wang, 2019). The Moderate Resolution Imaging Spectroradiometer (MODIS) has been acquiring reliable albedo imagery since 2000 (Schaaf & Wang, 2021). This study will use white-sky albedo acquired from MODIS. It is defined as the bihemispherical reflectance (completely diffuse) albedo and is the opposite extreme case to that of black-sky albedo, which is the directional hemispherical (direct beam) albedo (Schaaf et al., 2002). The true albedo can be derived using a combination of these (Schaaf et al., 2002), but due to the computational expense, white- and black-sky albedo have been used for research purposes where they provide an adequate approximate (e.g. Blok et al., 2011; Hovi et al., 2019; Plekhanova et al., 2022).

The pronounced warming in higher latitudes is expected to impact the vegetation in affected regions. Vegetation in colder regions is generally limited by temperature, and production is dependent on growing season length and warmth (Box et al., 2019; Hallinger et al., 2010; Higgins et al., 2023; Keenan & Riley, 2018). Due to warming, high latitude vegetation is displaying a decline in temperature limitation (Keenan & Riley, 2018). Mountainous areas in the northern hemisphere have also experienced amplified warming with a consequent impact on the alpine vegetation (Diaz et al., 2003). Studies record treeline advances both in latitudinal (toward poles) and altitudinal (uphill) directions in various locations around the globe (e.g. Bryn & Potthoff, 2018; Chapin et al., 2005; de Wit et al., 2014; Harsch et al., 2009; Rees et al., 2020). Rees et al. (2020) found that the treeline advance rate in high latitude regions is largest in western Eurasia, with circa 100 meters per year. Modelling has shown that the tree line in the Swedish mountains may advance at least 400 meters in elevation (Kullman & Kjällgren, 2008), or between 233 to 667 meters depending on location and climate scenario (Moen et al., 2004). This may cause a shrink of the alpine heaths in the Swedish Scandes (Kullman, 2010b; Moen et al., 2004), potentially with a reduction of up to 85% (Moen et al., 2004). Contrastingly, many studies have found an increase of shrub and tree growth in Scandinavian alpine areas

(Hallinger et al., 2010; Rundqvist et al., 2011; Wilson & Nilsson, 2009), as well as a decrease in species richness (Jonsson et al., 2021; Wilson & Nilsson, 2009), although another study has found indications of an increased biodiversity in the same region (Kullman, 2010b).

The terrestrial warming effect on vegetation has been demonstrated by increasing values in various vegetation indices, most commonly the Normalized Difference Vegetation Index (NDVI) (Bhatt et al., 2017; Blok et al., 2011; Box et al., 2019; Serreze & Barry, 2011) but also the Enhanced Vegetation Index (EVI) (Piao et al., 2020; Zhang et al., 2017). While vegetation indices do not measure any physical quality directly, they are typically used as proxies for various biochemical and biophysical qualities. NDVI is widely used partly due to its comparatively long record. However, unlike NDVI, EVI does not saturate in high biomass vegetated areas and is generally less sensitive to atmospheric contamination (Huete et al., 2002; Huete et al., 1999). NDVI uses the infrared and the red band, whereas EVI also uses the blue band as well as some additional coefficients. It is calculated as follows:

$$EVI = G\frac{N-R}{N+C_1R-C_2B+L} \qquad \text{Equation (1)}$$

Where N, R, and B are the near-infrared, red, and blue bands respectively. G is a gain factor, and L is a soil-adjustment factor which correct soil background brightness issues which limit NDVI to some extent. C_1 and C_2 are coefficients of aerosol resistance which corrects for aerosol influences on the red band (Huete et al., 1999). EVI typically ranges between 0 to 1 in vegetated areas, with more densely vegetated areas approaching 1 (Huete et al., 2002). This study will use EVI retrieved by MODIS, which has an EVI record dating back to 2000 (Didan, 2021).

The changes in vegetation described also have the potential to contribute to warming. Foley et al. (1994) reported that the expansion of boreal forests, with their typically low albedo, has the potential to give rise to a large positive climate warming feedback. Coincidentally, in higher latitudinal and altitudinal regions, summertime albedo is expected to decrease due to mountain birch forests replacing lighter-coloured vegetation such as lichens, graminoids, and mosses (de Wit et al., 2014; Ramtvedt et al., 2021). Chapin et al. (2005) reports that, while a shortening of the snow-free season length has had a large role in the arctic surface warming feedback, the increased absorption of radiation due to expansion of shrub and trees could potentially exceed this effect in the arctic and amplify atmospheric heating by two to seven times. This calls for an increased knowledge of vegetation and albedo dynamics in high latitude areas in order to predict future climate conditions. Furthermore, while most studies to date have focused on albedo dynamics during shoulder seasons where the impacts of changing snow cover are a focal point, an improved understanding of the same dynamics during growing season becomes increasingly important as the snow-free season becomes longer (Chapin et al., 2005).

1.2 Aim of study

This study aims to investigate whether the short-wave (SW) July albedo has significantly changed between 2000-2022 in the Swedish alpine region, and whether this correlates to a vegetation change, as quantified using the Enhanced Vegetation Index (EVI). It will do so by identifying, through remotely sensed data, (a) whether there is a decreasing trend in July SW albedo during this period, (b) if and how July EVI has changed in the same region, (c) if there is a significant relationship between July SW albedo and EVI during this period, and (d) how the trends are spatially distributed and if they differ between vegetation classes.

1.3 Study area

This study focuses on the Swedish portion of the Scandes, also termed the Scandinavian mountains, as well as its nearby areas of coniferous forests. A delineation of the area as well as its major vegetation classes can be viewed in Figure 1. The vegetation classes in this study are based on CORINE landcover (EEA, 2020), and this section will go into some detail on what these classes are characterised by for the Swedish alpine region in particular. The climate in the Scandes varies greatly depending on altitude, and thus the region can be loosely divided into three major vegetation zones: coniferous forests, birch forests, and tundra, which in this case is considered the area above the treeline (Rafstedt, 1984). These zones can be delineated according to altitude, as the lower regions have a generally temperate climate whereas the higher altitude regions can be compared to regions in the high arctic (Rafstedt, 1984). The zone borders, although not as clear-cut in nature as they are in theory, can vary by several hundred meters between the southern and northern parts of the Scandes due to the latitudinal impacts on the climate (Rafstedt, 1984).

The treeline in the Scandes is characterised by subalpine birch forest. The border of the treeline is typically determined by summer temperatures, which limits the alpine birch when summer temperatures gets too low. The treeline can be diffuse and is dependent on microclimates; clusters of trees can typically be found in sheltered conditions in the tundra zone above the general treeline (Rafstedt, 1984). This area corresponds with the broadleaf forest zone of Figure 1. The lower border of the birch forest zone also tends to be diffuse, with a soft transition between coniferous and birch trees (Rafstedt, 1984).

The study area covers a large portion of Sweden's coniferous forests. These are areas characterised by a tree layer with an understory of short woody ericaceous shrubs, mosses, and lichens (Nilsson & Wardle, 2005). Common tree species are Norway spruce (*Picea abies)* and Scots pine (*Pinus sylvestris)* (Linder et al., 1997). Wetlands are also common throughout the study area, typically in the forms of fens or bogs. Vegetation composition in these areas is characterised by mosses, dwarf shrubs, and graminoids (Jeglum et al., 2011). Wetlands are more common in the higher elevation portions of the boreal forest but does not as often appear above the treeline (Jeglum et al., 2011).

The tundra zone can be divided into low-, mid- and high-alpine zones, all with characteristic vegetation types. The low-alpine zone is characterised by shrubs, which tend to become shorter with increasing altitude due to decreasing temperatures and increasing wind exposure (Rafstedt, 1984). In the mid-alpine zone, the vegetation cover becomes discontinuous, with graminoids as the dominating vegetation type (Rafstedt, 1984). The high-alpine zone contains little vegetation, although some species can still be found, and is mostly characterised by block fields and perennial snow (Rafstedt, 1984). Moors and heathland as well as sparse vegetation are the two classes in Figure 1 which correspond with the tundra zone.

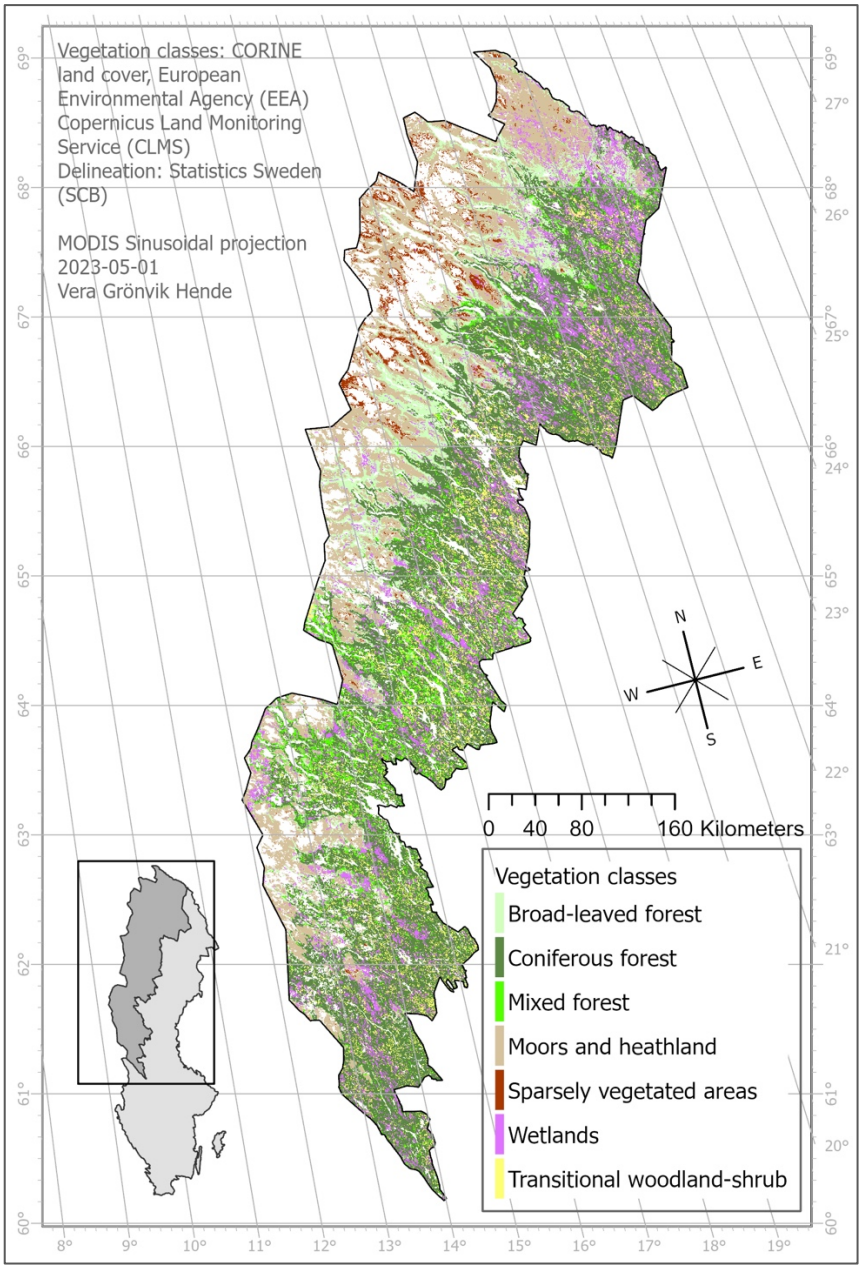

Figure. 1. Map of the study area and how the vegetation classes are distributed. Vegetation classes are derived from CORINE landcover (EEA, 2020). White areas indicate no data or pixels that have been filtered away due to land cover classes containing agricultural or non-vegetated areas.

2. Method

2.1 Data acquisition and processing

Both EVI and albedo values were obtained from Moderate Resolution Imaging Spectroradiometer (MODIS) data. Albedo values were obtained from the MODIS MCD43A3 v.061 product from the Land Processes (LP) Distributed Active Archive Center (DAAC) (Schaaf & Wang, 2021). This study used white-sky (whole diffuse bihemispherical reflectance) broadband shortwave albedo (hereinafter referred to using the acronym SWA) with 500 meters spatial resolution. The MCD43A3 product is produced daily and each image uses BRDF

information from the 16-day period that precedes and follows the image of interest. The July SWA for each year was calculated by taking the mean of SWA from all daily composite images from July 1st to 31st for each year during the 2000-2022 period. The MOD13A1 v.061 product, also distributed by the LP DAAC (Didan, 2021), was used to retrieve EVI values at 500 meters spatial resolution. The MOD13A1 product is produced as 16-days composites. The July EVI mean for each year was therefore calculated from three images each year, whose dates ranged from 26/6 to 12/8. Both the SWA and EVI products were Sinusoidally projected, as is standard for the MODIS data products. The calculation of means was done in ArcGIS Pro v.2.7.0 (Esri Inc., 2020).

The CORINE Land Cover (CLC) product (v.2020_20u1, raster format, 100 meters spatial resolution) was used for land cover data and was obtained from the European Union (EU) European Environment Agency (EEA) Copernicus Land Monitoring Service (CLMS) (EEA, 2020). The CLC product was projected into the Sinusoidal projection and resampled to a 500 meters spatial resolution using the nearest neighbour method in ArcGIS Pro v.2.7.0 (Esri Inc., 2020). It was then used to create a mask to remove water bodies and courses, urban areas, agricultural areas, bare rock, burnt areas, and permanent ice and snow, which was applied to the EVI and SWA July means to restrict the study to mostly vegetated pixels. The remaining classes in the CLC product were also used as an overlay to the SWA and EVI July means as a method to help identify the different vegetation classes. The remaining classes were coniferous forest, broadleaf forest, mixed forest, transitional woodland-shrub, natural grassland, moors and heathland, sparsely vegetated areas, and wetlands. Natural grassland and moors and heathland were combined into one category, hereinafter termed moors and heathland. Definitions for each vegetation class can be found in Kosztra et al. (2017).

2.2 Analysis

The SWA trend was quantified by fitting a linear regression model for each pixel, with year as the independent variable and July mean SWA as the dependent variable. The trend was derived from the linear slope as defined by the simple linear regression model $\hat{y} = a + bx$. The significance of the regression model was evaluated on a per pixel basis using the F-statistic, at a significance level of 0.05. The average change per year as a percentage was calculated by dividing the slope by the average albedo value for a given pixel and multiplying it by 100. These calculations were made in Excel v.16.54 (Microsoft, 2021). In ArcGIS Pro v.2.7.0 (Esri Inc., 2020), all pixels with an F-value below the critical F-statistic threshold (2.048, α=0.05) were filtered away to produce a map of only the pixels with significant change in SWA. This process was repeated for the EVI means, producing the same type of linear regression model for each pixel (year as independent variable, EVI as dependent, α=0.05) and then calculating the average EVI change per year in percent by dividing the slope of the regression model by the mean EVI for all years and multiplying it by 100.

The trend SWA and EVI variables created through linear regression were tested for normality using the Kolmogorov-Smirnov test in SPSS v.27 (IBM, 2020). The same software was used for all plots and correlation analysis. The division of vegetation classes was done using the CLC overlay. Both Pearson and Spearman correlations were tested between estimated trends of EVI (N_1=599848) and SWA (N_2=599848), as calculated from the linear regression described above. Additional Pearson and Spearman correlation analyses were also done for all vegetation classes separately with the same variables (EVI and SWA trends), as well as for the grouped vegetation classes of below treeline vegetation (including broadleaf forest, coniferous forest, mixed forest, and transitional woodland-shrub) and above treeline vegetation (including moors

and heathland and sparse vegetation). All correlation analysis was conducted using two-tailed tests.

In order to assess the fit of the linear regression on the SWA and EVI time series, a sample of each population of July means was taken. The sample size was calculated using Yamane's formula, specified as follows:

$$n = \frac{N}{1+N(e)^2} \qquad \text{Equation (2)}$$

Where n is the sample size, N is the population size (599848), and e is the desired level of precision (5%). The sample was taken by using the random points tool in ArcGIS Pro v.2.7.0 (Esri Inc., 2020). Time series for 2000-2022 were plotted in Excel v.16.54 (Microsoft, 2021) for each of the SWA and EVI July means in the sample. Outliers and irregular year-to-year fluctuations were detected visually and recorded by vegetation class.

3. Results

3.1 Albedo

The trends in SWA for July over a 23-year period (2000-2022) were calculated for the Swedish alpine region using a linear regression model. The SWA trend variable had a kurtosis of 43.89 and a Kolmogorov-Smirnov test determined that the variable was therefore not normally distributed. This study found that 44% of the area had significant ($p<0.05$) change in July SWA for this period. Out of the pixels that has had significant change in SWA, 79% were increasing trends, and 21% were decreasing trends. The spatial distribution of the average change per year in percent is displayed in Figure 2, along with the mean SWA for the entire period. The mean value for significant SWA trends was 0.00045 $year^{-1}$, with a mean standard error of 1.7e-6 $year^{-1}$ and a standard deviation of 0.00089 $year^{-1}$. Note that the standard deviation exceeds the mean, indicating that the spread is considerably large.

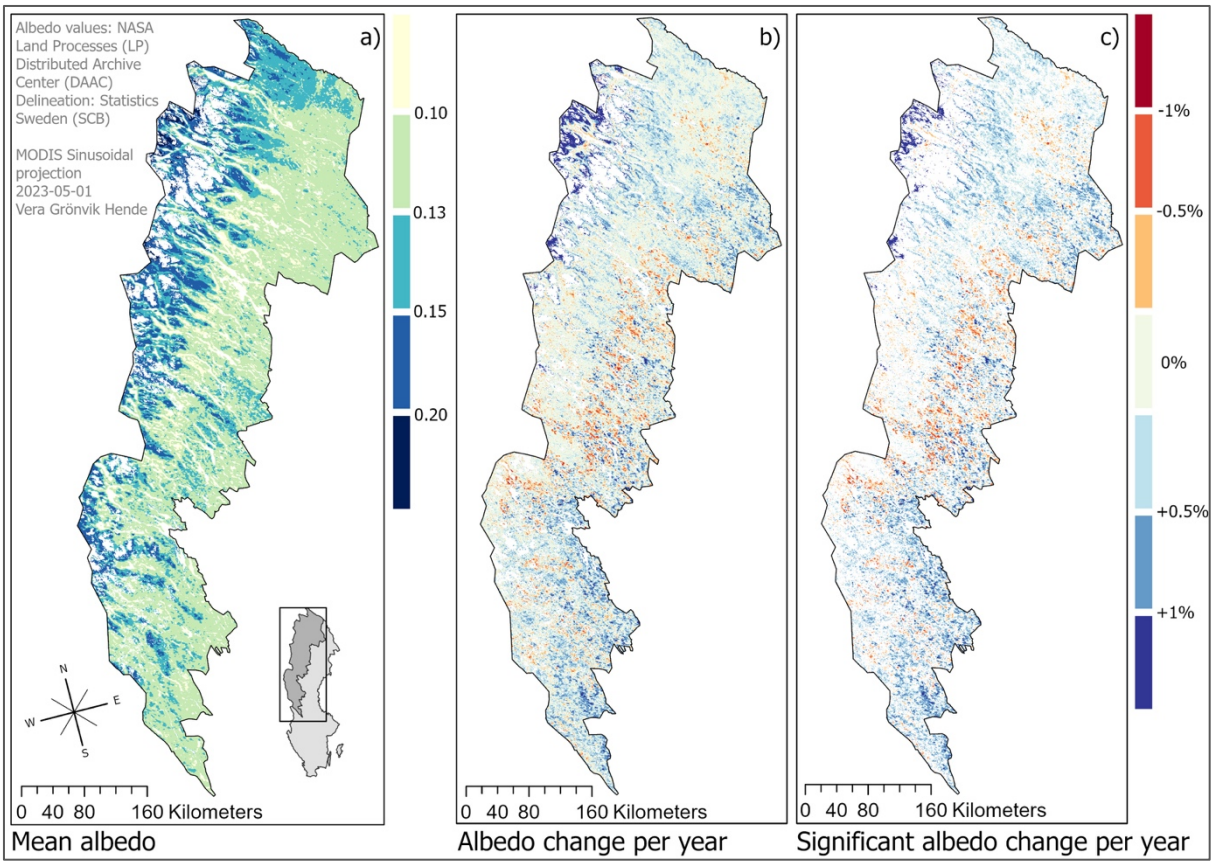

Figure 2. Spatial distribution of average shortwave albedo (SWA) values across the years 2000-2022 in the Swedish alpine region, derived from MODIS. Map a) shows the mean SWA for the time period. Map b) depicts the average change in SWA per year in percent, as estimated by a linear regression model, map c) shows the same as b) but only those pixels that had a significant ($p<0.05$) relationship between SWA and year. White areas indicate no data or pixels that have been filtered away.

3.2 EVI

Change in EVI was estimated for the years 2000-2022 in the Swedish alpine region through linear regression. The variable of EVI trend was not normally distributed, as determined by a Kolmogorov-Smirnov test. It had a kurtosis of 2.26. About a third (32%) of the area had a significant ($p<0.05$) change in EVI, the majority of which (80%) were increasing trends. The spatial distribution of the average change per year in percent, as well as the mean absolute EVI values, are displayed in Figure 3. The mean value for the significant EVI trends was 0.00171 year^{-1}, with a standard error mean of 5.7e-6 year^{-1} and a standard deviation of 0.00246 year^{-1}.

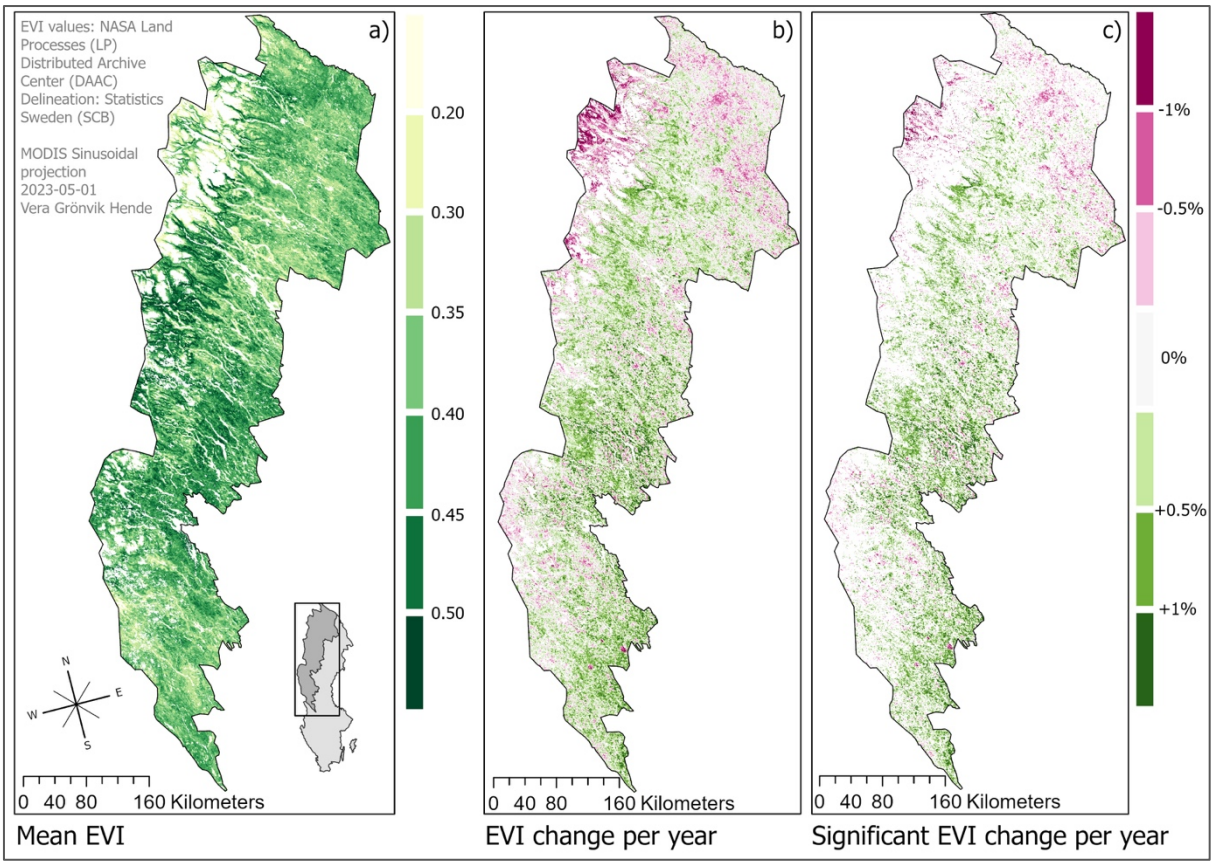

Figure 3. Spatial distribution of average Enhanced Vegetation Index (EVI) values across the years 2000-2022 in the Swedish alpine region, derived from MODIS. Map a) shows the mean EVI for the time period. Map b) depicts the average change in EVI per year in percent, as estimated by a linear regression model, map c) shows the same but only those pixels that had a significant ($p<0.05$) relationship between EVI and year. White areas indicate no data or pixels that have been filtered away.

3.3 Albedo and EVI relationship

Out of the pixels that had a significant change in SWA, 38% also had a significant change in EVI, most of which were increasing trends (83%). The estimated change per year in SWA is plotted against the estimated change per year in EVI in Figure 4. Pearson's r between the variables was computed as -0.004 ($p=0.002$) with a 95% confidence interval of -0.006 – -0.001, indicating that there was no linear relationship between the variables. This result was also supported by the shape of the scatterplot in Figure 4, which revealed two distinct clusters with seemingly opposite relationships. One cluster held below-treeline vegetation (mixed, coniferous, and broadleaf forest), and the other contained above-treeline vegetation (moors and heathland, and sparse vegetation). The non-linear appearance, as well as the non-normal distribution of the data motivated the use of Spearman's rho, which determined a significant ($p<0.001$), although quite weak, positive monotonic relationship ($\rho=0.227$, (0.225 – 0.230)).

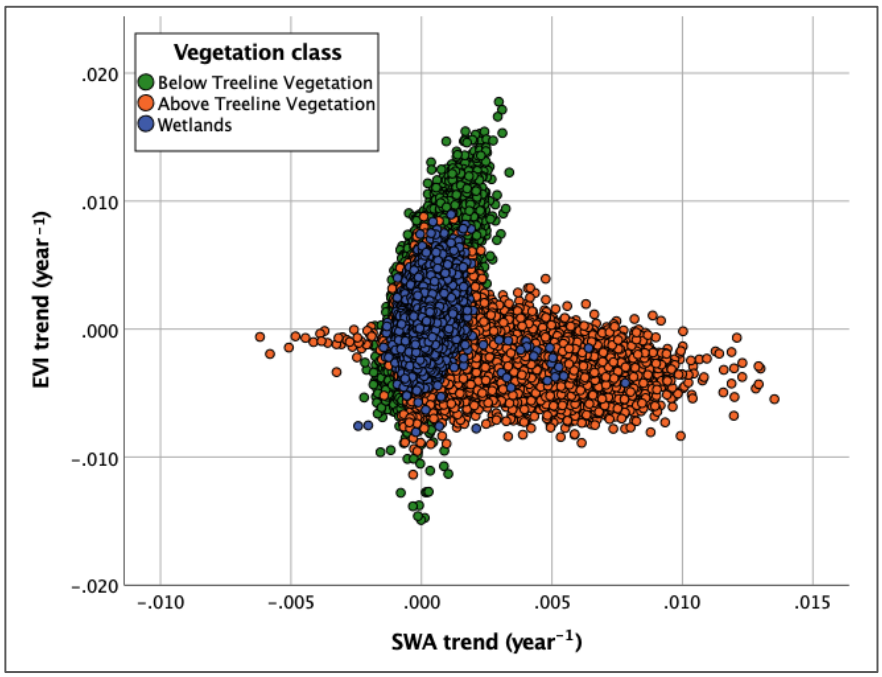

Figure 4. The estimated change per year (linear regression slope coefficients) of shortwave albedo (SWA) against the estimated change per year (linear regression slope coefficients) of the Enhanced Vegetation Index (EVI) in the Swedish alpine region between the years 2000-2022. Identified in the scatterplot are vegetation classes based on CORINE landcover (EEA, 2020), here divided into three broader classes; below treeline vegetation (mixed forest, broadleaf forest, coniferous forest, and transitional woodland-shrub), above treeline vegetation (moors and heathland, and sparse vegetation), and wetlands.

3.4 Vegetation class comparison

The means and standard deviations of the estimated trends for the pixels for which both SWA and EVI trends were significant are categorized by vegetation class in Figure 5. All below treeline vegetation classes (transitional woodland-shrub, and broadleaf, mixed, and coniferous forest), along with wetlands, have a higher mean EVI trend than SWA trend. Broadleaf and coniferous forests have very similar values compared to the other vegetation classes. Broadleaf forest has a mean significant SWA trend of 0.00039 year^{-1} (standard error mean = 4e-6 year^{-1}, standard deviation = 0.00038 year^{-1}) and coniferous forest 0.00040 year^{-1} (standard error mean = 2e-6 year^{-1}, standard deviation = 0.00051 year^{-1}). The mean SWA trend for mixed forest however approaches zero (mean = 0.00007 year^{-1}, standard error mean = 8e-6 year^{-1}, standard deviation = 0.00062 year^{-1}), indicating a similar distribution of positive and negative changes in SWA for mixed forest.

Note that the standard deviation is higher for EVI trends than SWA trends in almost all cases, only excluding sparse vegetation which has a similarly large spread for both variables. Sparse vegetation is the only vegetation class with a negative mean EVI (mean = -0.00138 year^{-1}, standard error mean = 0.00008 year^{-1}, standard deviation = 0.00306 year^{-1}), but the standard deviation exceeds into positive values, indicating that the change in EVI for this vegetation class has a large spread and may differ considerably throughout the area. While the above treeline vegetation classes follow the same pattern of higher SWA than EVI trends, their values differ substantially. While the SWA and EVI trends are quite similar for moors and heathland, the difference in trends is pronounced for sparse vegetation. Indeed, the SWA trend is highest for sparse vegetation out of all vegetation classes, with a mean of 0.00348 year^{-1} (standard error mean = 0.00008 year^{-1}, standard deviation = 0.00300 year^{-1}).

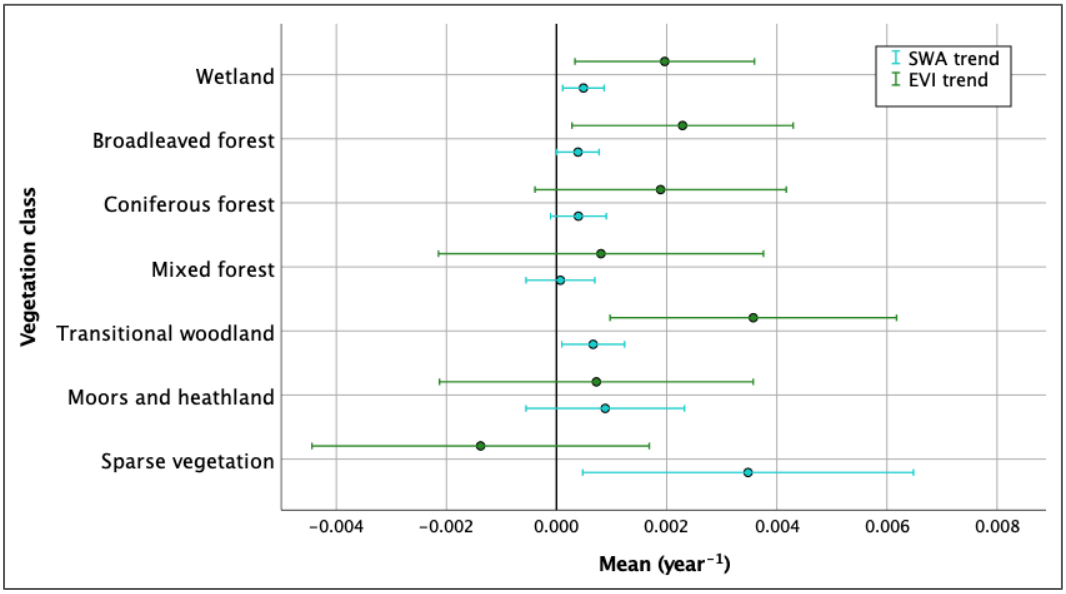

Figure 5. Means and standard deviations for the significant trends (linear regression slope coefficients) in shortwave albedo (SWA) (blue) and Enhanced Vegetation Index (EVI) (green) between the years 2000-2022 for each vegetation class identified in the Swedish alpine region. The plot uses a confidence interval of 95% for the means. Vegetation classes are derived from CORINE Landcover (EEA, 2020).

Similar to the plot in Section 3.3, scatterplots were also produced for the vegetation classes separately, as well as Pearson and Spearman correlation coefficients for the SWA and EVI trends. The coefficients and their corresponding p-values and confidence intervals are displayed in Table 1. All correlation analyses found significant correlations, but this can be attributed to the large sample sizes (N>10 000 for all cases). The Pearson coefficients are generally higher than Spearman, but the Spearman coefficients may be considered as the more reliable measure of correlation in this case due to the non-normality of the data. The strongest Spearman correlation was found to be for the sparse vegetation class, followed by transitional woodland-shrub.

Table 1. Correlation coefficients and their corresponding p-values and confidence intervals for all vegetation classes included in this study, as based on CORINE landcover (EEA, 2020), including the larger groups of below- and above treeline vegetation. The below treeline vegetation includes the classes broadleaf forest, coniferous forest, mixed forest, and transitional woodland-shrub. The above treeline vegetation includes the classes moors and heathland, and sparse vegetation.

Vegetation class	**Pearson coefficient**	**Pearson confidence interval (95%)**	**Spearman coefficient**	**Spearman confidence interval (95%)**
Wetlands	0.256 (p<0.001)	0.250 – 0.263	0.253 (p<0.001)	0.247 – 0.260
Below treeline vegetation (all)	0.443 (p<0.001)	0.440 – 0.445	0.387 (p<0.001)	0.384 – 0.390
Broadleaf forest	0.274 (p<0.001)	0.267 – 0.281	0.258 (p<0.001)	0.250 – 0.265
Coniferous forest	0.419 (p<0.001)	0.416 – 0.423	0.373 (p<0.001)	0.370 – 0.377
Mixed forest	0.439 (p<0.001)	0.430 – 0.447	0.400 (p<0.001)	0.391 – 0.409
Transitional woodland-shrub	0.495 (p<0.001)	0.488 – 0.503	0.460 (p<0.001)	0.452 – 0.468
Above treeline vegetation (all)	-0.380 (p<0.001)	-0.384 – -0.375	-0.129 (p<0.001)	-0.134 – -0.123
Moors and heathland	-0.296 (p<0.001)	-0.302 – -0.295	-0.045 (p<0.001)	-0.050 – -0.039
Sparse vegetation	-0.647 (p<0.001)	-0.656 – 0.637	-0.608 (p<0.001)	-0.619 – -0.598

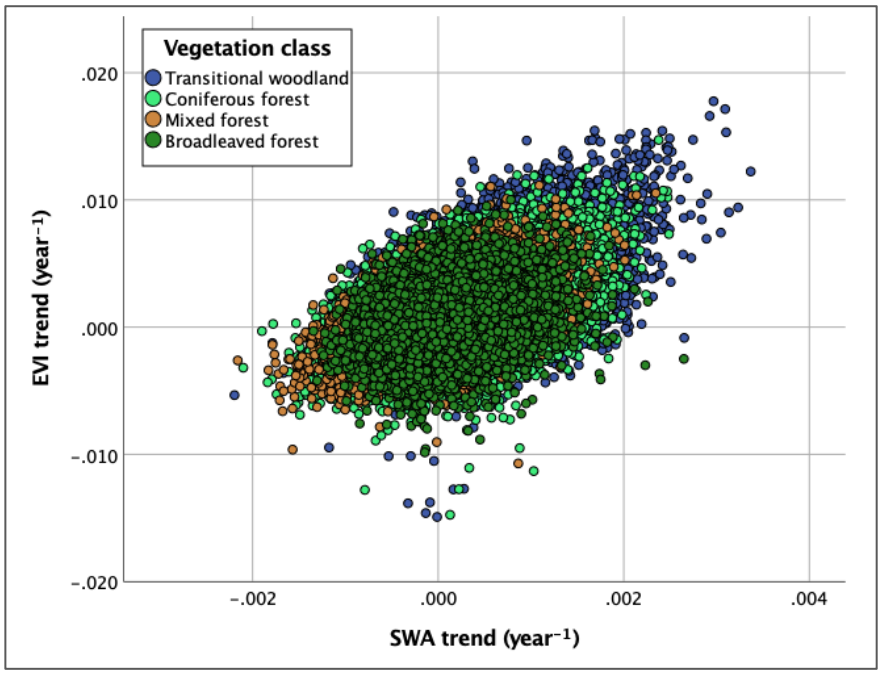

*Figure 6. The estimated change per year (linear regression slope coefficients) of shortwave albedo (SWA trend) against the estimated change per year (linear regression slope coefficients) of the Enhanced Vegetation Index (EVI trend), in the Swedish alpine region between the years 2000-2022 for the four **below treeline** vegetation classes; mixed forest, coniferous forest, broadleaf forest, and transitional woodland-shrub.*

The below treeline vegetation had the most linear distribution (see Figure 6), which is reflected in the comparative similarities between the Pearson and Spearman coefficients for those vegetation classes. Wetlands (Figure 7) follow a similar distribution to the below treeline vegetation but has a portion of values which are spread out and to some extent could be argued to follow the same pattern as that of the above treeline vegetation (compare with Figure 8).

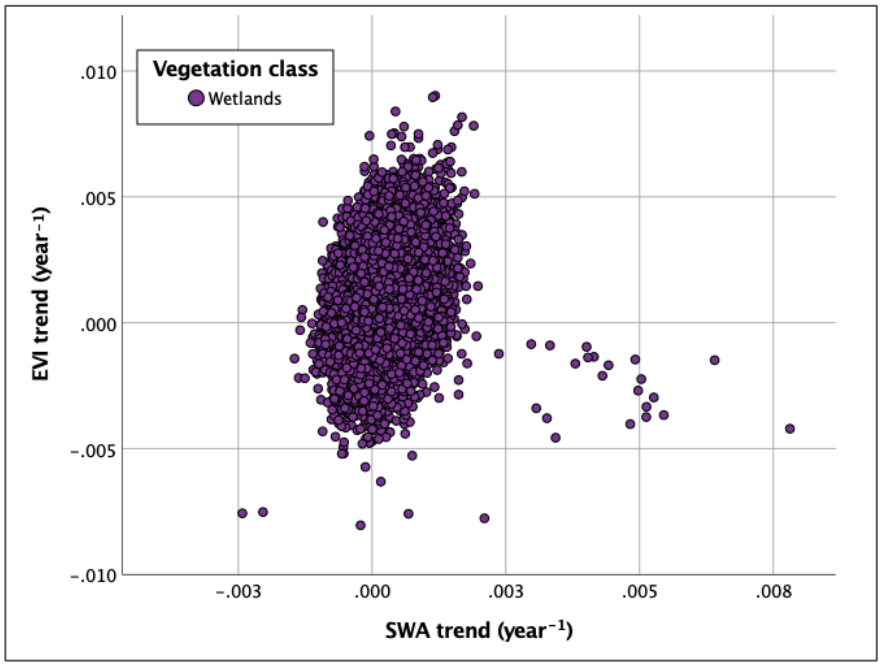

*Figure 7. The estimated change per year (linear regression slope coefficients) of shortwave albedo (SWA trend) against the estimated change per year (linear regression slope coefficients) of the Enhanced Vegetation Index (EVI trend), for the **wetland** vegetation class in the Swedish alpine region between the years 2000-2022.*

The scatterplot of the above treeline vegetation (Figure 8) indicates two different clusters, with one following a similar distribution to the below treeline vegetation with a positive relationship, and the other following a negative relationship between the SWA and EVI trends. It could also be an indication of another type of relationship; it bears some similarities to a negative logarithmic distribution. The nonlinear relationship is somewhat reflected in the linear Pearson coefficient being higher than the monotonic Spearman coefficient, which is close to zero. This low number seems to be largely influenced by the weak correlation of the moors and heathland class ($\rho = -0.045$). Contrastingly, the sparse vegetation class had the strongest correlation of all vegetation classes ($r = -0.647$ and $\rho = -0.608$).

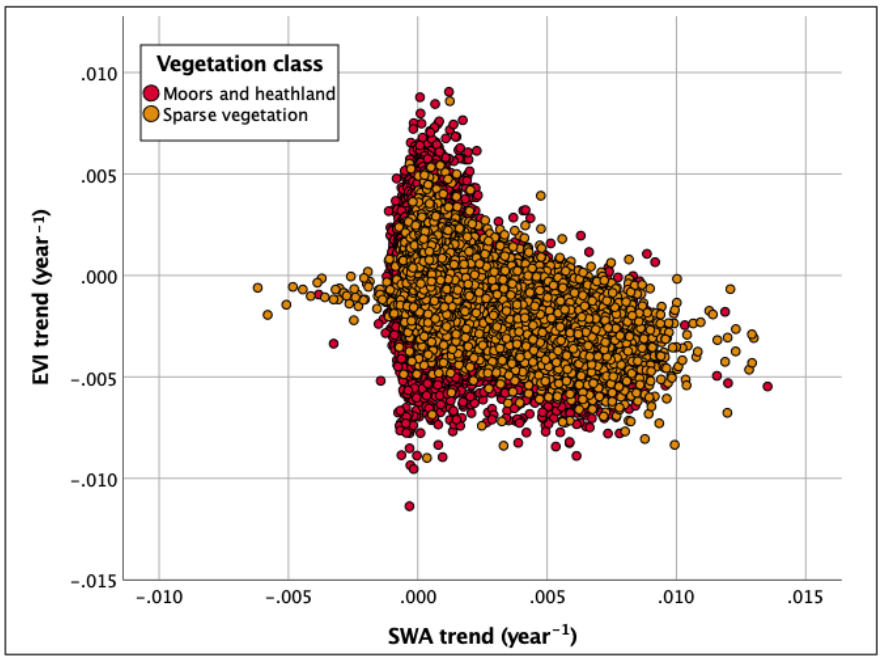

Figure 8. The estimated change per year (linear regression slope coefficients) of shortwave albedo (SWA trend) against the estimated change per year (linear regression slope coefficients) of the Enhanced Vegetation Index (EVI trend), in the Swedish alpine region between the years 2000-2022 for the two ***above treeline*** *vegetation classes; sparse vegetation, and moors and heathland.*

3.5 Time series outlier evaluation

A sample size of n=400 was taken from the SWA and EVI July means for each year within the period 2000-2022. 6.3% of the SWA time series had at least one outlier, and 15.8% had irregular year-to-year fluctuations. While moors and heathland held the largest percentage of total outliers (56%), this is not necessarily representative for the class as the vegetation classes were not of equal size within the sample. The vegetation class that held the highest percentage of outliers within its class was sparse vegetation (80%) but this may not be entirely representative either as the total number of sparse vegetation pixels within the sample was comparatively low ($n_{sparse} = 5$). Figure 9a depicts one such time series where two outliers were found in a sparse vegetation SWA time series. Moors and heathland had the next-to-highest percentage of outliers within its vegetation class sample (17.5%, $n_{moors\&heathland} = 80$). The lowest percentage of SWA outliers within its vegetation class sample was coniferous forests (1.1%, $n_{coniferous} = 178$), except for transitional woodland-shrub, which had zero outliers within the sample ($n_{woodland\text{-}shrub} = 22$). The vegetation class that had the largest portion of irregular fluctuations within its time series was broadleaf forest (27%, $n_{broadleaf} = 37$), closely followed by moors and heathland (23.8%). Figure 9b depicts one of the broadleaf forest time series with irregular year-to-year fluctuations.

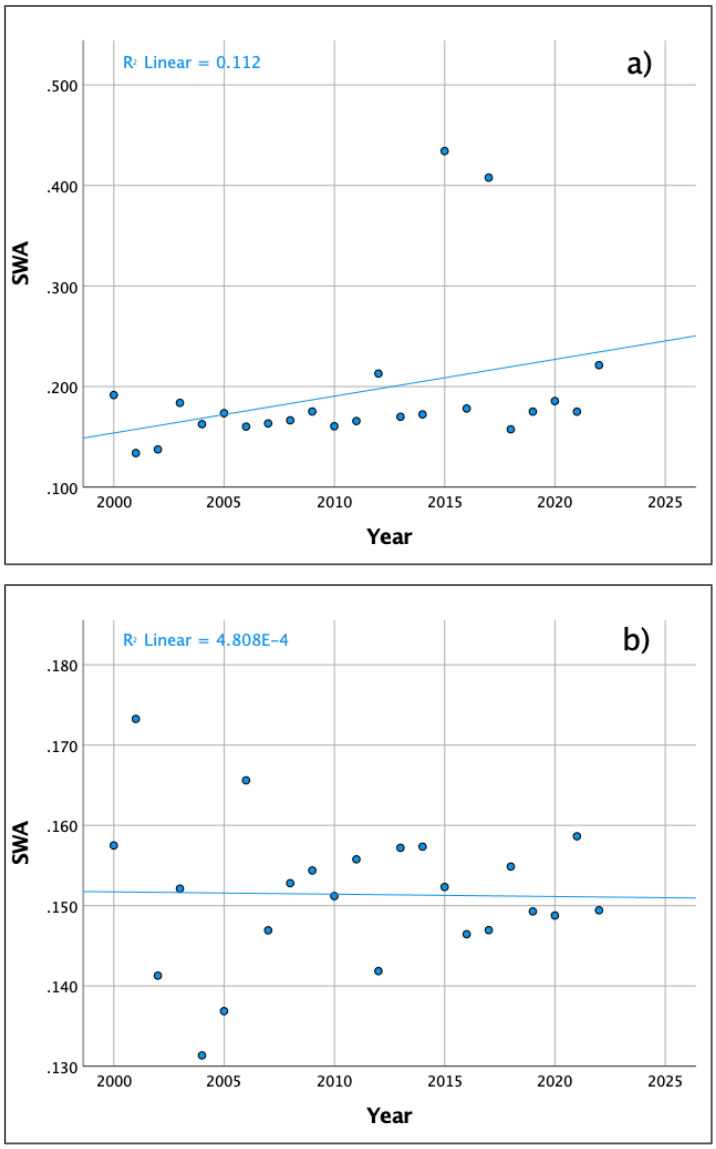

Figure 9. Examples of the plotted shortwave albedo (SWA) time series from the sample. Time series a) depicts the SWA values of a pixel with the sparse vegetation class and is an example of a time series where outliers were found. The outliers are in this case in the years 2015 and 2017. Time series b) depicts an example of a SWA broadleaf forest time series with irregular year-to-year fluctuations. All values are means from July of each year.

The EVI time series had a higher portion of outliers (8.0%) and a lower portion of irregular year-to-year fluctuations (3.8%) than the SWA time series. Sparse vegetation was again the vegetation class with the highest percentage of outliers (20%), followed by mixed forest (13%), and broadleaf forest (11%). Transitional woodland-shrub had again zero outliers. Wetlands had the next to smallest portion of EVI outliers (4.8%, $n_{wetlands} = 63$). The vegetation class that had the highest percentage of irregular EVI year-to-year fluctuations within its class was sparse vegetation (20%), followed by moors and heathland (10%). See Figure 10 for examples of EVI time series with one outlier (Figure 10a) and irregular year-to-year fluctuations (Figure 10b). These plots both represent what was typical for each type of outlier detection classification (single outlier or irregular year-to-year fluctuations). All n values are the same for EVI as for SWA, as the same sample was taken for both variables. As can be observed in Figures 9 and 10, these outliers may have impacted the regression slopes, and thus the trend variables, substantially.

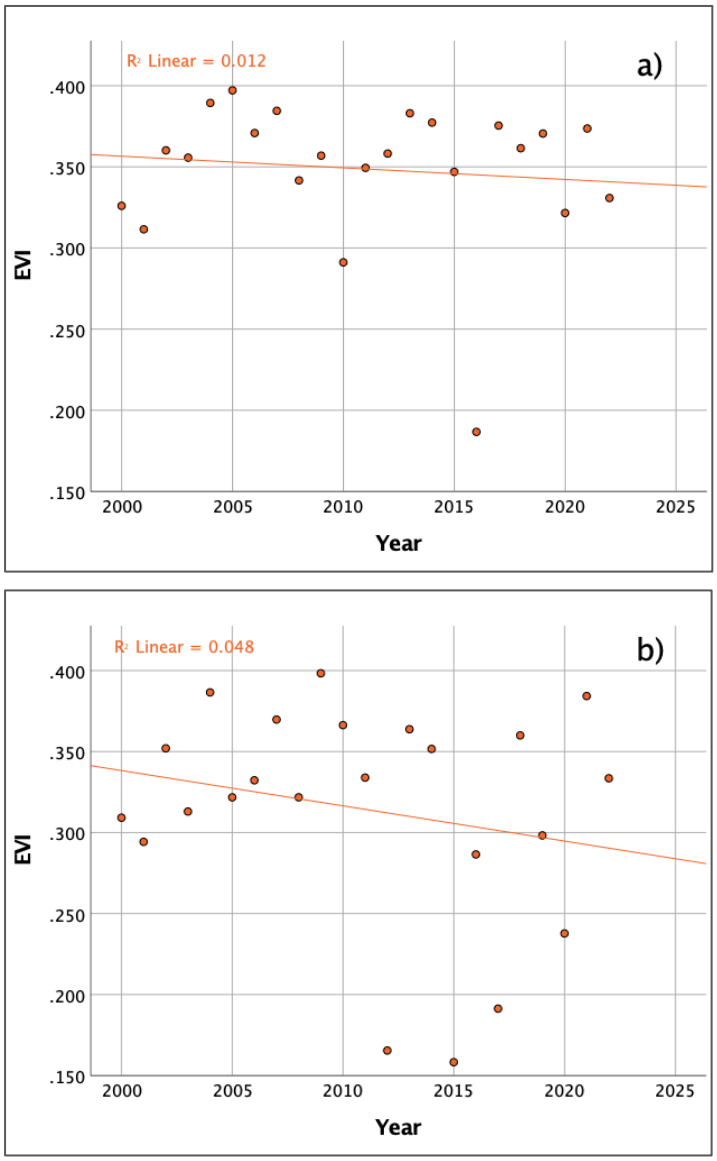

Figure 10. Examples of the plotted Enhanced Vegetation Index (EVI) time series from the sample. Time series a) depicts the EVI values of a pixel with the coniferous forest vegetation class and is an example of where an outlier was found. The outlier in this case is in the year 2016. Time series b) is an example where irregular year-to-year fluctuations were found, in this case in a pixel with the vegetation class moors and heathland. All values are means from July of each year.

4. Discussion

4.1 Albedo and EVI were mostly stable or increasing

Despite indications that a warmer climate would correspond with a vegetation increase (Box et al., 2019; Hallinger et al., 2010; Serreze & Barry, 2011) and a corresponding decrease in albedo for both the coniferous forests and the tundra regions (Chapin et al., 2005; Foley et al., 1994; Ramtvedt et al., 2021), this study found no significant SWA changes in 56% of the study area, and for the 44% of the area with significant changes, the majority (79%) were increases. These are similar results as those of Plekhanova et al. (2022), who found that the SWA was mostly stable or had increased in the arctic between 2000 to 2021. They discussed that the SWA increase to some extent could be attributed to lighter vegetation replacing darker soil as the vegetation climbed northward higher into the arctic, as previously found by Alessandri et

al. (2021). Alessandri et al. (2021) also found that the surface albedo feedback in the northern hemisphere tends to be negative in regions were vegetation dominates. This corresponds to the findings of this study, especially for the below treeline vegetation where an increase in EVI correlated with an increase in SWA, which would imply a negative surface albedo feedback.

The narrative of lighter vegetation replacing darker soils may be attributed to some areas of the tundra regions of the Swedish Scandes. However, the results of this study found a negative correlation between SWA and EVI for the above treeline vegetation. While this study found a SWA increase in these areas, the EVI was decreasing in some regions of the above treeline areas, which is contrary to what several previous studies have found indications of, which is that vegetation has increased in the Scandes over the two recent decades (Hallinger et al., 2010; Løkken et al., 2020; Rundqvist et al., 2011; Wilson & Nilsson, 2009). Some studies have however also found indications of browning trends – that is, a decrease in vegetation – in northern hemisphere alpine areas (Barredo et al., 2020) and arctic tundra (Lara et al., 2018; Myers-Smith et al., 2020; Phoenix & Bjerke, 2016). This might provide an explanation for the negative EVI trends in the above treeline vegetation that were found in this study.

However, a differentiation must be made here between the sparse vegetation class and the moors and heathland class. The moors and heathland class, corresponding to the low- and to some extent the medium alpine zone as delineated by Rafstedt (1984), have a much weaker correlation between SWA and EVI trends than the sparsely vegetated zone. The EVI was mostly increasing for moors and heathland, and for those areas the narrative of lighter vegetation replacing darker soils could perhaps be applied. However, the variability of the EVI trend both being positive and negative for the tundra regions implies that there is a high complexity for the affected species and their temperature responses. This corresponds with the findings of other studies that the growth trends for tundra is highly heterogenous and varies greatly depending on species (Dobbert et al., 2021; Elmendorf et al., 2012; Myers-Smith et al., 2020). A clear relationship between EVI and SWA in the above treeline vegetation can therefore not be determined without looking more closely at the individual species affected.

Sparse vegetation mostly experienced a SWA increase along with a decrease in EVI. These results are the opposite of the study's hypothesis of an EVI increase and a SWA decrease. As discussed above, this does not correspond with the findings of previous studies that found an increase of vegetation in the high alpine areas of the Scandes (Hallinger et al., 2010; Rundqvist et al., 2011). However, as previously mentioned, tundra regions have also shown browning trends in some areas which could explain the decrease in EVI. The corresponding SWA increase could be explained by the exposed soil having a comparatively high albedo; this would be valid if the soil is dry, as dry soils typically have a higher albedo than wet soils (Yang et al., 2020). Furthermore, the appearance of the scatterplot for the above treeline vegetation indicates a threshold where the SWA and EVI relationship shifts from positive to negative. This holds true for both the sparse vegetation class as well as for moors and heathland. This implies a hidden factor within this relationship which may either be due to some climatic factor such as aspect or precipitation, or due to differences between the individual species within the classes. However, some care must be taken when interpreting these results, especially with regard to the sparse vegetation class as this was the class with the largest proportion of outliers within the time series evaluation sample. The sparse vegetation class is mainly situated in regions highly affected by rough terrain and snow which in some years may persist in July even for those pixels that were not labelled as perennial snow by the landcover class layer. These shortcomings will be further discussed in Section 4.4.

This study found that coniferous forests experienced mostly an increase in SWA as well as EVI for 2000 to 2022. This contrasts the findings by previous studies that a coniferous forest expansion should correspond with a decrease in albedo due to their inherently dark colouring and thus lesser reflective properties (Foley et al., 1994). The contradictory findings of this study suggest that the SWA is highly affected by other factors in the coniferous forest that this study did not cover. Albedo has been proven to decrease with increasing tree height (Kuusinen et al., 2016; Webster & Jonas, 2018), growing stock (Kuusinen et al., 2016), stand biomass (Lukeš et al., 2013) and age (Kuusinen et al., 2016; Webster & Jonas, 2018). Forest management procedures in the boreal forest, such as thinning and logging, may therefore alter their albedo due to the forest composition changes (Lukeš et al., 2013), and thereby act as a masking factor to the otherwise expected effects from climate warming. However, a forest thinning would be expected to correlate with a decrease in EVI, as it would implicate a decrease in vegetation density. The mechanisms for the trends for the coniferous forest found in this study are therefore particularly ambiguous and calls for an increased understanding of the changes within the boreal coniferous forests and its effects on albedo.

The changes in both SWA and EVI for the region were, for the majority of the region, not significant. While a range of studies suggest treeline advances in the Scandes (Kullman, 2002, 2010a; Ramtvedt et al., 2021), these higher altitude establishments of tree species may not be indicative of an overall treeline advance throughout the region. While temperature-limited, the findings of several studies indicate that the rate of treeline advance for mountain birch is not as large as temperature increases should have caused were it the only limiting factor (Cairns et al., 2011; Løkken et al., 2020; Mienna et al., 2022). Herbivory has been found as a major masking factor with respect to mountain birch advances otherwise expected from climate warming (Cairns et al., 2011; Hofgaard et al., 2010; Scharn et al., 2022), along with nitrogen limitation (Scharn et al., 2021). In addition, a recent study suggests that treeline advance rates in the subarctic are not as large as previously thought (Rees et al., 2020). The findings of (Harsch et al., 2009) also suggest similar patterns for the forests close to the Scandes, within which the treeline has been stable for the last 100 years. This could explain the relatively low proportion of the area that had any significant changes in EVI (32%).

The same narrative described for coniferous forest could perhaps be applied for mixed forest, although this was one of the vegetation classes with a comparatively high proportion of SWA decreases. As this study does not cover individual species and local changes, the explanation for the SWA changes within this vegetation class is difficult to ascertain. It is likely due to regional species differences and local changes in the affected areas. Some explanations could be attributed to forest management practices here, much like the case of coniferous forests, as well as differences in stand age and canopy structure. Similar difficulties can be applied to the transitional woodland-shrub, although additional complications can be applied here as well. The transitional woodland-shrub is defined by CORINE landcover (CLC) as "transitional bushy and herbaceous vegetation with occasional scattered trees" (Kosztra et al., 2017), which can for example be attributed to clear-cut areas (Kosztra et al., 2017). This causes problems in terms of the temporal period: What may be defined as a transitional woodland-shrub in 2017-2018, which is the temporal extent of the CLC product (EEA, 2020), may not be classed as the same type of vegetation 18 years earlier. Of course, similar reasoning should also be considered for the rest of the vegetation classes. The SWA and EVI trends for transitional woodland-shrub are, however, different enough from the coniferous forest region that they should not be grouped into one class. The higher EVI trend for this class for example suggests that the vegetation is growing at a faster rate here, which may be attributed to these areas not being as 'saturated' with vegetation as compared to coniferous forests.

Lastly, the albedo increase could be attributed to factors not directly affected by vegetation cover, such as soil moisture. As mentioned briefly above, surface albedo and soil moisture have a linear relationship as reported by previous studies, with lower soil moisture corresponding to a higher albedo (Roxy et al., 2010; Yang et al., 2020). It is not however clear whether the soil moisture has changed significantly in the study area. Scharn et al. (2021) have reported that increased warming and earlier snowmelt tend to decrease soil moisture in tundra ecosystems, while Löffler (2007) on the other hand found that the soil moisture has been stable in the Scandes. Furthermore, much of the high alpine region of the Swedish Scandes is characterised by block fields and thus do not have larger patches of soil (Rafstedt, 1984), and thus any changes in soil moisture may not explain the extent of albedo increase found in this study.

4.2 Albedo and EVI correlations

This study found a weak positive Spearman correlation between the trends in SWA and EVI for the study area (ρ=0.227) and a Pearson coefficient approaching zero (r = -0.004). As previously mentioned in Section 3, this indicates no clear relationship between the two variables and warrants a closer look at each vegetation class. Furthermore, as the data was both non-normally distributed as well as largely nonlinear, the Spearman coefficients should be given larger emphasis than the Pearson coefficients calculated in this study. The Pearson coefficients however provide some value as they provide an understanding of the differing linearities of the correlation between the different vegetation classes. For example, the below treeline vegetation grouped class has similar Pearson and Spearman coefficients compared to the above treeline vegetation class, which had a large difference between Pearson and Spearman coefficients and was distributed along a less linear distribution according to their scatterplots (compare Figures 6 and 8). What should also be considered for the correlation analysis is that all of the correlations were significant likely due to the large sample size and thus emphasis should not be put on the significance here but rather on the individual correlation coefficients. For example, the Spearman coefficient for the moors and heathland class is almost zero and thus we cannot make any assumptions there about any clear relationship between SWA and EVI. In this case it is perhaps even more likely than the other vegetation classes that other factors have a larger role and that there are considerable differences between unknown variables within the vegetation class itself.

Furthermore, the negative correlation for the above treeline vegetation classes, especially the sparse vegetation class, could be attributed to varying snow conditions. While snowmelt could have been a factor, the EVI and SWA trends actually correspond with what would rather indicate an increase in snow-covered areas in summer (increasing SWA and decreasing EVI for most of the sparsely vegetated areas), which again contradicts previous findings for tundra regions (Chapin et al., 2005; Hallinger et al., 2010; Serreze & Barry, 2011). As discussed above, this change could also be attributed to browning trends which would provide an explanation for the findings of this study in regard to the high-alpine areas experiencing a decrease in EVI in some areas. What should again be brought up here is the larger proportion of outliers for the above-treeline areas which may have disturbed the data and caused the contradictory trends in EVI and SWA. The above treeline areas also have generally higher standard deviations and mean standard errors than the rest of the vegetation classes, which further decreases the sturdiness of these findings.

4.3 Method limitations

A simple linear regression was used to produce the trend variables in this study which was used for all correlation analysis. Therefore, some emphasis must be put on the fit of a linear regression to the SWA and EVI values as this then greatly impacted the final results. Firstly, a simple linear regression may not be deemed an ideal model for regional changes in a landscape, as they are rarely strictly linear. A generalised additive model (Webb et al., 2021) or Theil-Sen's slope (Plekhanova et al., 2022) are two examples used by similar studies which may have provided a better fit. However due to the time constraints of this study, a simple linear model was determined to be the most appropriate in this particular case. Would more time and resources have been available another type of slope should have been applied. The problems with the simple linear regression model were further illuminated in the sample time series evaluation, whose results are presented in Section 3.5. It found that the time series rarely followed a linear slope, in some cases with irregular fluctuations year-to-year. This may have resulted in poor trend estimations, which would then have multiplied into the correlation analysis and result interpretation. Furthermore, the sample time series evaluation revealed outliers which may have greatly impacted the trends. Ideally these outliers should have been filtered out at an earlier stage before the trend variables were produced. Due to the large population along with the time constraints this was however not deemed feasible, and as a result all trend variables should be interpreted with caution. However, while the linear regression model causes some limitations in the interpretation of the results, they could still be considered an adequate estimate within the constraints of this study.

This study uses MODIS data with 500 meters spatial resolution. This is rather coarse data, which restricts the study in several ways. This study cannot take into account any local differences within the vegetation, nor any species-specific changes. Since the study does not account for the occurrence of specific species, it cannot investigate the complex relationships between species and specific species changes which may have attributed to the results of this study, and thus only discuss the changes in SWA and EVI at a more general level. As per the results of Kuusinen et al. (2014), a finer resolution satellite dataset such as Landsat is able to detect more detailed information on forest albedo than MODIS. Due to the coarse resolution, this study fails to take into account many of the differences at a regional scale which is bound to occur within the study area. Most notable are the differences in growing season length between the northern and southern parts of the study area. There is an approximate 9° latitudinal difference between the northern- and southernmost points in the study, which is likely to affect at what seasonal stage the vegetation is in during July throughout the region. While not quite as impactful in the region with coniferous forests, it is of higher importance for the above treeline vegetation as well as the broadleaf forest region which is characterised by alpine birch (Rafstedt, 1984), which are both highly temperature limited (Box et al., 2019; Hallinger et al., 2010; Higgins et al., 2023; Keenan & Riley, 2018). These areas are therefore likely to be in different stages of blooming throughout the study area, which poses a problem for the division of vegetation classes in this study, which did not take into account the latitudinal difference. This may have produced unreliable results throughout the region.

The vegetation near and above the treeline is also affected by topographical and aspect differences. The establishment of mountain birch is often dependent on favourable microclimates, such as south-facing slopes or slopes and valleys sheltered from wind (Rafstedt, 1984; Sundqvist et al., 2008). These are variabilities that may not be effectively represented in the coarse-scale resolution used in this study. The same issue may be applied to species-specific responses to changes in the climate and landscape. Some species may be more vulnerable to

herbivory than others, for example, and the expansion of one species may impact another in various ways. Scharn et al. (2022) suggest that forest advances in high latitudes are indeed not linear, but dependent on the responses of individual species. Any such changes within one vegetation class defined in this study is difficult to identify. A finer data resolution may have provided insights in the complexities of the heterogenous landscape of which the Swedish alpine region is characterised by (Kullman, 2010a; Rafstedt, 1984). This study may also have benefited from an inclusion of elevation and aspect as additional variables, although it may not have produced significant results at the available MODIS resolution (500 meters).

Since both variables analysed in this study are derived from the same satellite, they are both vulnerable to the same technical issues which may have occurred in the satellite measurements. As both SWA and EVI are based upon data collected by the same satellite, any faulty measurements on the different wavelengths may not have been detected. Known issues are for example that the MCD43A3 MODIS albedo product can produce less reliable results in rough terrain with steep slopes (Wen et al., 2022), and the MOD13A1 MODIS EVI product may exhibit erratic behaviour over snow covered surfaces (Didan et al., 2015). These are both factors that are expected to occur in the study area, most notably in the higher alpine regions. Low values for EVI could for example have been influenced by persisting snow cover in the high-altitude regions, resulting in possibly false indications of very low vegetation cover. Coincidentally, the above treeline vegetation, which would have theoretically been impacted the most by this, contain the vegetation classes that had the most outliers within the sample taken for the time series evaluation. As a result, the results for these variables have less reliability than those of the below treeline vegetation.

4.4 Considerations for future studies

While this study was limited to two variables (SWA and EVI), an inclusion of additional variables would have increased an understanding of the factors affecting an albedo change or stability. This is highlighted by the generally weak correlations between the SWA and EVI trends, as well as the differing clusters in the scatterplots produced in the study, which all suggest that other variables may have a significant impact upon the albedo. As previously discussed, factors connecting to the canopy complexities of the vegetation, topography and aspect, or even soil moisture may have provided insight on the results produced here. Fire occurrence is another variable which may have provided further insights, as reported in a study focused on albedo changes in the arctic-boreal region (Webb et al., 2021). Furthermore, an inclusion of the surface temperature throughout the area would have been valuable to include in order to illuminate to what extent the temperature may have increased, along with whether a possible temperature increase differed significantly between the different regions in the study area.

Any future studies on this topic may also consider including data for the entire year. Due to time limitations, this study only covered the month of July as this was considered an adequate representation of the peak conditions found in the summer period. However, a study covering the entire year would give a better estimate of the entire growing season, as well as the land surface albedo variability in the shoulder seasons which have been previously recorded in primarily the arctic (Crook & Forster, 2014; Loranty et al., 2014). Furthermore, a similar study for the winter months would shed a light on the albedo variability due to a changing snow cover. While this study found an increase in shortwave albedo in July, it is possible that this increase does not significantly affect the changes in albedo throughout the entire year as the albedo is likely to have experienced a decrease during winter and shoulder season months,

according to the seasonal snow cover decrease in the northern hemisphere reported by previous studies (Edwards et al., 2007; Folland et al., 2001).

5. Conclusion

In contrast to expectations, the July shortwave albedo (SWA) has been largely stable or even increased in the Swedish alpine region between the years 2000-2022. The July EVI has correspondingly been stable or increased, although the sparse vegetation of the high alpine region deviates from this result, with some regions experiencing a decrease in EVI, indicating browning trends. The correlation between the changes in SWA and EVI for the entire region as a whole is weak and demonstrate a need for a closer look at local vegetation processes. The correlations between the EVI and SWA trends varied substantially between each vegetation class, and it seems clear that factors affecting the SWA are a result of differing dynamics specific to each region. The varying correlation strength in the SWA and EVI trends between different vegetation classes indicates that the dynamic between vegetation growth and albedo differs substantially throughout different vegetation types, and that no generalisations should be made for the entire region as a whole. The mechanisms for changes in SWA and EVI in July for areas both above and below the treeline remain ambiguous and could be attributed to species-specific responses. Studies investigating the species composition and responses at a finer scale have the potential to illuminate the specific albedo dynamics for each subregion within the Swedish alpine region.

6. References

Alessandri, A., Catalano, F., De Felice, M., Hurk, B., & Balsamo, G. (2021). Varying snow and vegetation signatures of surface albedo feedback on the Northern Hemisphere land warming. *Environmental Research Letters*, *16*. https://doi.org/10.1088/1748-9326/abd65f

Barredo, J. I., Mauri, A., & Caudullo, G. (2020). Alpine Tundra Contraction under Future Warming Scenarios in Europe. *Atmosphere*, *11*(7).

Bhatt, U., Walker, D., Raynolds, M., Bieniek, P., Epstein, H., Comiso, J., Pinzon, J., Tucker, C., Steele, M., Ermold, W., & Zhang, J. (2017). Changing seasonality of panarctic tundra vegetation in relationship to climatic variables. *Environmental Research Letters*, *12*, 055003. https://doi.org/10.1088/1748-9326/aa6b0b

Blok, D., Schaepman-Strub, G., Bartholomeus, H., Heijmans, M. M. P. D., Maximov, T., & Berendse, F. (2011). The response of Arctic vegetation to the summer climate: Relation between shrub cover, NDVI, surface albedo and temperature. *Environmental Research Letters*, *6*, 035502. https://doi.org/10.1088/1748-9326/6/3/035502

Box, J., Colgan, W., Christensen, T. R., Schmidt, N., Lund, M., Parmentier, F.-J., Brown, R., Bhatt, U., Euskirchen, E., Romanovsky, V., Walsh, J., Overland, J., Wang, M., Corell, R., Meier, W., Wouters, B., Mernild, S., Mård, J., Pawlak, J., & Olsen, M. (2019). Key indicators of Arctic climate change: 1971–2017. *Environmental Research Letters*, *14*, 045010. https://doi.org/10.1088/1748-9326/aafc1b

Bryn, A., & Potthoff, K. (2018). Elevational treeline and forest line dynamics in Norwegian mountain areas – a review. *Landscape Ecology*, *33*(8), 1225-1245. https://doi.org/10.1007/s10980-018-0670-8

Cairns, D. M., Granberg, T. C., Lafon, C. W., Young, A. B., & Moen, J. (2011). Scandinavian Treelines are Impacted by Herbivory. *AGU Fall Meeting Abstracts*. https://ui.adsabs.harvard.edu/abs/2011AGUFM.B12B..02C

Chapin, F. S., Sturm, M., Serreze, M. C., McFadden, J. P., Key, J. R., Lloyd, A. H., McGuire, A. D., Rupp, T. S., Lynch, A. H., Schimel, J. P., Beringer, J., Chapman, W. L., Epstein, H. E., Euskirchen, E. S., Hinzman, L. D., Jia, G., Ping, C. L., Tape, K. D., Thompson, C. D. C., Walker, D. A., & Welker, J. M. (2005). Role of Land-Surface Changes in Arctic Summer Warming. *Science*, *310*(5748), 657-660. https://doi.org/10.1126/science.1117368

Cohen, J., Screen, J. A., Furtado, J. C., Barlow, M., Whittleston, D., Coumou, D., Francis, J., Dethloff, K., Entekhabi, D., Overland, J., & Jones, J. (2014). Recent Arctic amplification and extreme mid-latitude weather. *Nature Geoscience*, *7*(9), 627-637. https://doi.org/10.1038/ngeo2234

Crook, J. A., & Forster, P. M. (2014). Comparison of surface albedo feedback in climate models and observations. *Geophysical Research Letters*, *41*(5), 1717-1723. https://doi.org/https://doi.org/10.1002/2014GL059280

de Wit, H. A., Bryn, A., Hofgaard, A., Karstensen, J., Kvalevåg, M. M., & Peters, G. P. (2014). Climate warming feedback from mountain birch forest expansion: reduced albedo dominates carbon uptake. *Global Change Biology*, *20*(7), 2344-2355. https://doi.org/https://doi.org/10.1111/gcb.12483

Diaz, H. F., Eischeid, J. K., Duncan, C., & Bradley, R. S. (2003). Variability of Freezing Levels, Melting Season Indicators, and Snow Cover for Selected High-Elevation and Continental Regions in the Last 50 Years. *Climatic Change*, *59*(1), 33-52. https://doi.org/10.1023/A:1024460010140

Didan, K. (2021). *MODIS/Terra Vegetation Indices 16-Day L3 Global 500m SIN Grid V061* [Data set]. NASA EOSDIS Land Processes DAAC. Retrieved April 21, 2023 from https://doi.org/10.5067/MODIS/MOD13A1.061

Didan, K., & Barreto-Muñoz, A. (2019). MODIS Vegetation Index User's Guide (MOD13 Series), Collection 6.1. University of Arizona. https://lpdaac.usgs.gov/documents/621/MOD13_User_Guide_V61.pdf

Dobbert, S., Pape, R., & Löffler, J. (2021). Contrasting growth response of evergreen and deciduous arctic-alpine shrub species to climate variability. *Ecosphere*, *12*(8). https://doi.org/https://doi.org/10.1002/ecs2.3688

Edwards, A. C., Scalenghe, R., & Freppaz, M. (2007). Changes in the seasonal snow cover of alpine regions and its effect on soil processes: A review. *Quaternary International*, *162-163*, 172-181. https://doi.org/https://doi.org/10.1016/j.quaint.2006.10.027

Elmendorf, S. C., Henry, G. H. R., Hollister, R. D., Björk, R. G., Bjorkman, A. D., Callaghan, T. V., Collier, L. S., Cooper, E. J., Cornelissen, J. H. C., Day, T. A., Fosaa, A. M., Gould, W. A., Grétarsdóttir, J., Harte, J., Hermanutz, L., Hik, D. S., Hofgaard, A., Jarrad, F., Jónsdóttir, I. S., Keuper, F., Klanderud, K., Klein, J. A., Koh, S., Kudo, G., Lang, S. I., Loewen, V., May, J. L., Mercado, J., Michelsen, A., Molau, U., Myers-Smith, I. H., Oberbauer, S. F., Pieper, S., Post, E., Rixen, C., Robinson, C. H., Schmidt, N. M., Shaver, G. R., Stenström, A., Tolvanen, A., Totland, Ø., Troxler, T., Wahren, C.-H., Webber, P. J., Welker, J. M., & Wookey, P. A. (2012). Global assessment of experimental climate warming on tundra vegetation: heterogeneity over space and time. *Ecology Letters*, *15*(2), 164-175. https://doi.org/https://doi.org/10.1111/j.1461-0248.2011.01716.x

European Environment Agency (EEA). (2020). *Corine Land Cover (CLC) 2018* (Version 2020_20u1) [Data set]. Copernicus Land Monitoring Service. Retrieved April 21, 2023 from https://land.copernicus.eu/pan-european/corine-land-cover/clc2018

Foley, J. A., Kutzbach, J. E., Coe, M. T., & Levis, S. (1994). Feedbacks between climate and boreal forests during the Holocene epoch. *Nature*, *371*(6492), 52-54. https://doi.org/10.1038/371052a0

Folland, C., Karl, T., Christy, J., Clarke, R., Gruza, G., Jouzel, J., Mann, M., Oerlemans, J., Salinger, M., & Wang, S. (2001). Observed climate variability and change. *Climate change*, *2001*, 99.

Hallinger, M., Manthey, M., & Wilmking, M. (2010). Establishing a missing link: warm summers and winter snow cover promote shrub expansion into alpine tundra in Scandinavia. *New Phytologist*, *186*(4), 890-899. https://doi.org/https://doi.org/10.1111/j.1469-8137.2010.03223.x

Harsch, M. A., Hulme, P. E., McGlone, M. S., & Duncan, R. P. (2009). Are treelines advancing? A global meta-analysis of treeline response to climate warming. *Ecology Letters*, *12*(10), 1040-1049. https://doi.org/https://doi.org/10.1111/j.1461-0248.2009.01355.x

Higgins, S. I., Conradi, T., & Muhoko, E. (2023). Shifts in vegetation activity of terrestrial ecosystems attributable to climate trends. *Nature Geoscience*, *16*(2), 147-153. https://doi.org/10.1038/s41561-022-01114-x

Hofgaard, A., Løkken, J. O., Dalen, L., & Hytteborn, H. (2010). Comparing warming and grazing effects on birch growth in an alpine environment – a 10-year experiment. *Plant Ecology & Diversity*, *3*(1), 19-27. https://doi.org/10.1080/17550871003717016

Hovi, A., Lindberg, E., Lang, M., Arumäe, T., Peuhkurinen, J., Sirparanta, S., Pyankov, S., & Rautiainen, M. (2019). Seasonal dynamics of albedo across European boreal forests: Analysis of MODIS albedo and structural metrics from airborne LiDAR. *Remote*

Sensing of Environment, *224*, 365-381. https://doi.org/https://doi.org/10.1016/j.rse.2019.02.001
Huete, A., Didan, K., Miura, T., Rodriguez, E. P., Gao, X., & Ferreira, L. G. (2002). Overview of the radiometric and biophysical performance of the MODIS vegetation indices. *Remote Sensing of Environment*, *83*(1), 195-213. https://doi.org/https://doi.org/10.1016/S0034-4257(02)00096-2
Huete, A., Justice, C., & Van Leeuwen, W. (1999). MODIS vegetation index (MOD13). *Algorithm theoretical basis document*, *3*(213), 295-309.
Jeglum, J., Sandring, S., Christensen, P., Glimskär, A., Allard, A., Nilsson, L., & Svensson, J. (2011). Main Ecosystem Characteristics and Distribution of Wetlands in Boreal and Alpine Landscapes in Northern Sweden Under Climate Change. In O. Grillo and G. Venora (eds.), *Ecosystem Biodiversity* (pp. 193-218). InTech. https://doi.org/10.5772/25066
Jonsson, B., Dahlgren, J., Ekström, M., Esseen, P.-A., Grafström, A., Ståhl, G., & Westerlund, B. (2021). Rapid Changes in Ground Vegetation of Mature Boreal Forests—An Analysis of Swedish National Forest Inventory Data. *Forests*, *12*, 475. https://doi.org/10.3390/f12040475
Keenan, T. F., & Riley, W. J. (2018). Greening of the land surface in the world's cold regions consistent with recent warming. *Nature Climate Change*, *8*(9), 825-828. https://doi.org/10.1038/s41558-018-0258-y
Kosztra, B., Büttner, G., Hazeu, G., & Arnold, S. (2017). Updated CLC illustrated nomenclature guidelines. *European Environment Agency: Wien, Austria*, 1-124.
Kullman, L. (2002). Rapid recent range-margin rise of tree and shrub species in the Swedish Scandes. *Journal of Ecology*, *90*(1), 68-77. https://doi.org/https://doi.org/10.1046/j.0022-0477.2001.00630.x
Kullman, L. (2010a). One century of treeline change and stability: experiences from the Swedish scandes [article]. *Landscape Online*, *17*(1), 1-31. https://doi.org/10.3097/LO.201017
Kullman, L. (2010b). A Richer, Greener and Smaller Alpine World: Review and Projection of Warming-Induced Plant Cover Change in the Swedish Scandes. *AMBIO*, *39*(2), 159-169. https://doi.org/10.1007/s13280-010-0021-8
Kullman, L., & Kjällgren, L. (2008). Holocene pine tree-line evolution in the Swedish Scandes: Recent tree-line rise and climate change in a long-term perspective. *Boreas*, *35*, 159-168. https://doi.org/10.1111/j.1502-3885.2006.tb01119.x
Kuusinen, N., Stenberg, P., Korhonen, L., Rautiainen, M., & Tomppo, E. (2016). Structural factors driving boreal forest albedo in Finland. *Remote Sensing of Environment*, *175*, 43-51. https://doi.org/https://doi.org/10.1016/j.rse.2015.12.035
Kuusinen, N., Tomppo, E., Shuai, Y., & Berninger, F. (2014). Effects of forest age on albedo in boreal forests estimated from MODIS and Landsat albedo retrievals. *Remote Sensing of Environment*, *145*, 145-153. https://doi.org/https://doi.org/10.1016/j.rse.2014.02.005
Lara, M. J., Nitze, I., Grosse, G., Martin, P., & McGuire, A. D. (2018). Reduced arctic tundra productivity linked with landform and climate change interactions. *Scientific Reports*, *8*(1), 2345. https://doi.org/10.1038/s41598-018-20692-8
Liang, S., & Wang, J. (2019). *Advanced remote sensing: terrestrial information extraction and applications*. Academic Press.
Linder, P., Elfving, B., & Zackrisson, O. (1997). Stand structure and successional trends in virgin boreal forest reserves in Sweden. *Forest Ecology and Management*, *98*(1), 17-33. https://doi.org/https://doi.org/10.1016/S0378-1127(97)00076-5

Löffler, J. (2007). The influence of micro-climate, snow cover, and soil moisture on ecosystem functioning in high mountains. *Journal of Geographical Sciences*, *17*(1), 3-19. https://doi.org/10.1007/s11442-007-0003-3

Løkken, J. O., Evju, M., Söderström, L., & Hofgaard, A. (2020). Vegetation response to climate warming across the forest–tundra ecotone: species-dependent upward movement. *Journal of Vegetation Science*, *31*(5), 854-866. https://doi.org/https://doi.org/10.1111/jvs.12911

Loranty, M. M., Berner, L. T., Goetz, S. J., Jin, Y., & Randerson, J. T. (2014). Vegetation controls on northern high latitude snow-albedo feedback: observations and CMIP5 model simulations. *Global Change Biology*, *20*(2), 594-606. https://doi.org/https://doi.org/10.1111/gcb.12391

Lukeš, P., Stenberg, P., & Rautiainen, M. (2013). Relationship between forest density and albedo in the boreal zone. *Ecological Modelling*, *261-262*, 74-79. https://doi.org/https://doi.org/10.1016/j.ecolmodel.2013.04.009

Mienna, I. M., Austrheim, G., Klanderud, K., Bollandsås, O. M., & Speed, J. D. M. (2022). Legacy effects of herbivory on treeline dynamics along an elevational gradient. *Oecologia*, *198*(3), 801-814. https://doi.org/10.1007/s00442-022-05125-8

Moen, J., Aune, K., Edenius, L., & Angerbjörn, A. (2004). Potential Effects of Climate Change on Treeline Position in the Swedish Mountains. *Ecology and Society*, *9*. https://doi.org/10.5751/ES-00634-090116

Myers-Smith, I. H., Kerby, J. T., Phoenix, G. K., Bjerke, J. W., Epstein, H. E., Assmann, J. J., John, C., Andreu-Hayles, L., Angers-Blondin, S., Beck, P. S. A., Berner, L. T., Bhatt, U. S., Bjorkman, A. D., Blok, D., Bryn, A., Christiansen, C. T., Cornelissen, J. H. C., Cunliffe, A. M., Elmendorf, S. C., Forbes, B. C., Goetz, S. J., Hollister, R. D., de Jong, R., Loranty, M. M., Macias-Fauria, M., Maseyk, K., Normand, S., Olofsson, J., Parker, T. C., Parmentier, F.-J. W., Post, E., Schaepman-Strub, G., Stordal, F., Sullivan, P. F., Thomas, H. J. D., Tømmervik, H., Treharne, R., Tweedie, C. E., Walker, D. A., Wilmking, M., & Wipf, S. (2020). Complexity revealed in the greening of the Arctic. *Nature Climate Change*, *10*(2), 106-117. https://doi.org/10.1038/s41558-019-0688-1

Nilsson, M. C., & Wardle, D. A. (2005). Understory vegetation as a forest ecosystem driver: evidence from the northern Swedish boreal forest. *Frontiers in Ecology and the Environment*, *3*(8), 421-428. https://doi.org/https://doi.org/10.1890/1540-9295(2005)003[0421:UVAAFE]2.0.CO;2

Phoenix, G. K., & Bjerke, J. W. (2016). Arctic browning: extreme events and trends reversing arctic greening. *Global Change Biology*, *22*(9), 2960-2962. https://doi.org/https://doi.org/10.1111/gcb.13261

Piao, S., Wang, X., Park, T., Chen, C., Lian, X., He, Y., Bjerke, J. W., Chen, A., Ciais, P., Tømmervik, H., Nemani, R. R., & Myneni, R. B. (2020). Characteristics, drivers and feedbacks of global greening. *Nature Reviews Earth & Environment*, *1*(1), 14-27. https://doi.org/10.1038/s43017-019-0001-x

Pithan, F., & Mauritsen, T. (2014). Arctic amplification dominated by temperature feedbacks in contemporary climate models. *Nature Geoscience*, *7*(3), 181-184. https://doi.org/10.1038/ngeo2071

Plekhanova, E., Kim, J.-S., Oehri, J., Erb, A., Schaaf, C., & Schaepman-Strub, G. (2022). Mid-summer snow-free albedo across the Arctic tundra was mostly stable or increased over the past two decades. *Environmental Research Letters*, *17*(12), 124026. https://doi.org/10.1088/1748-9326/aca5a1

Rafstedt, T. (1984). *FJALLENS VEGETATION Jämtlands län: En översikt av Jämtlandsfjällens vegetation baserad på vegetationskartering och naturvärdering.* Naturvårdsverket. http://urn.kb.se/resolve?urn=urn:nbn:se:naturvardsverket:diva-7478

Ramtvedt, E. N., Bollandsås, O. M., Næsset, E., & Gobakken, T. (2021). Relationships between single-tree mountain birch summertime albedo and vegetation properties. *Agricultural and Forest Meteorology*, *307*, 108470. https://doi.org/https://doi.org/10.1016/j.agrformet.2021.108470

Rees, W. G., Hofgaard, A., Boudreau, S., Cairns, D. M., Harper, K., Mamet, S., Mathisen, I., Swirad, Z., & Tutubalina, O. (2020). Is subarctic forest advance able to keep pace with climate change? *Global Change Biology*, *26*(7), 3965-3977. https://doi.org/https://doi.org/10.1111/gcb.15113

Roxy, M. S., Sumithranand, V. B., & Renuka, G. (2010). Variability of soil moisture and its relationship with surface albedo and soil thermal diffusivity at Astronomical Observatory, Thiruvananthapuram, south Kerala. *Journal of Earth System Science*, *119*(4), 507-517. https://doi.org/10.1007/s12040-010-0038-1

Rundqvist, S., Hedenås, H., Sandström, A., Emanuelsson, U., Eriksson, H., Jonasson, C., & Callaghan, T. V. (2011). Tree and Shrub Expansion Over the Past 34 Years at the Tree-Line Near Abisko, Sweden. *AMBIO*, *40*(6), 683-692. https://doi.org/10.1007/s13280-011-0174-0

Schaaf, C., Gao, F., Strahler, A., Lucht, W., Li, X., Tsang, T., Strugnell, N., Zhang, X., Jin, Y., Muller, J. P., Lewis, P., Barnsley, M., Hobson, P., Disney, M., Roberts, G., Dunderdale, M., Doll, C., d'Entremont, R., Hu, B., & Roy, D. (2002). First operational BRDF, albedo nadir reflectance products from MODIS. *Remote Sensing of Environment*, *83*, 135-148. https://doi.org/10.1016/S0034-4257(02)00091-3

Schaaf, C., & Wang, Z. (2021). *MODIS/Terra+Aqua BRDF/Albedo Daily L3 Global - 500m V061* [Data set]. NASA EOSDIS Land Processes DAAC. Retrieved April 21, 2023 from https://doi.org/10.5067/MODIS/MCD43A3.061

Scharn, R., Little, C., Bacon, C., Alatalo, J., Antonelli, A., Björkman, M., Molau, U., Nilsson, R. H., & Björk, R. (2021). Decreased soil moisture due to warming drives phylogenetic diversity and community transitions in the tundra. *Environmental Research Letters*, *16*, 064031. https://doi.org/10.1088/1748-9326/abfe8a

Scharn, R., Negri, I. S., Sundqvist, M. K., Løkken, J. O., Bacon, C. D., Antonelli, A., Hofgaard, A., Nilsson, R. H., & Björk, R. G. (2022). Limited decadal growth of mountain birch saplings has minor impact on surrounding tundra vegetation. *Ecology and Evolution*, *12*(6), e9028. https://doi.org/https://doi.org/10.1002/ece3.9028

Serreze, M. C., & Barry, R. G. (2011). Processes and impacts of Arctic amplification: A research synthesis. *Global and Planetary Change*, *77*(1), 85-96. https://doi.org/https://doi.org/10.1016/j.gloplacha.2011.03.004

Statistics Sweden. (2018). *Demographic Statistical Areas*. [Data set]. Retrieved April 17, 2023 from https://www.scb.se/en/services/open-data-api/open-geodata/deso--demographic-statistical-areas/

Sundqvist, M. K., Björk, R. G., & Molau, U. (2008). Establishment of boreal forest species in alpine dwarf-shrub heath in subarctic Sweden. *Plant Ecology & Diversity*, *1*(1), 67-75. https://doi.org/10.1080/17550870802273395

Webb, E., Loranty, M., & Lichstein, J. (2021). Surface water, vegetation, and fire as drivers of the terrestrial Arctic-boreal albedo feedback. *Environmental Research Letters*, *16*. https://doi.org/10.1088/1748-9326/ac14ea

Webster, C., & Jonas, T. (2018). Influence of canopy shading and snow coverage on effective albedo in a snow-dominated evergreen needleleaf forest. *Remote Sensing of Environment*, *214*, 48-58. https://doi.org/https://doi.org/10.1016/j.rse.2018.05.023

Wen, J., Lin, X., Wu, X., Bao, Y., You, D., Gong, B., Tang, Y., Wu, S., Xiao, Q., & Liu, Q. (2022). Validation of the MCD43A3 Collection 6 and GLASS V04 Snow-Free Albedo Products Over Rugged Terrain. *IEEE Transactions on Geoscience and Remote Sensing*, *60*, 1-11. https://doi.org/10.1109/TGRS.2022.3214103

Wilson, S. D., & Nilsson, C. (2009). Arctic alpine vegetation change over 20 years. *Global Change Biology*, *15*(7), 1676-1684. https://doi.org/https://doi.org/10.1111/j.1365-2486.2009.01896.x

Yang, J., li, Z., Zhai, P., Zhao, Y., & Gao, X. (2020). The influence of soil moisture and solar altitude on surface spectral albedo in arid area. *Environmental Research Letters*, *15*. https://doi.org/10.1088/1748-9326/ab6ae2

Zhang, Y., Song, C., Band, L. E., Sun, G., & Li, J. (2017). Reanalysis of global terrestrial vegetation trends from MODIS products: Browning or greening? *Remote Sensing of Environment*, *191*, 145-155. https://doi.org/https://doi.org/10.1016/j.rse.2016.12.018